DIVISION S-6—SOIL & WATER MANAGEMENT & CONSERVATION

Tillage-Induced Spatial Distribution of Surface Crusts on a Sandy Paleustult from Togo

C. L. Bielders, P. Baveye,* L. P. Wilding, L. R. Drees, and C. Valentin

ABSTRACT

The spatial distribution of crusts in coarse-textured soils and the processes affecting it are poorly documented, despite the potential impact of crusts on water infiltration. This study addresses the influence of tillage-induced microrelief on the morphology and spatial distribution of surface crusts in an Oxic Paleustult from southern Togo (West Africa). Replicate 1-m^2 plots were exposed to 217 mm of natural rainfall during a 6-wk period, during which the surface topography was measured three times. Subsequently, 24 undisturbed crust samples were used for micromorphological analysis. The crusts exhibited a range of morphologies but were nevertheless adequately mapped and characterized according to two main types. Type 1 crusts (≈runoff crusts) showed several superposed clay bands, 100 to 500 mm thick, buried within a micromass-depleted sand layer ≤12 mm thick. Type 2 crusts (≈erosion crusts) had an exposed clay band a few tenths of a millimeter thick. The spatial distribution of crusts at the time of sampling appeared better correlated with the initial than with the final microtopography of the plots. These findings suggest that crust distribution should be regarded as history dependent and that erosion and deposition processes largely governed the development of the crusts. This latter aspect is in agreement with the recent crust genesis model of Valentin and Bresson, as is the fact that clay bands in our plots were laterally continuous at all observational scales ≤0.1 m. Other mechanisms proposed in the literature for the development of clay bands did not seem able to account adequately for the observed pattern.

RESEARCH during the last three decades has established that a wide range of soils may develop a surface crust under the influence of rainfall (Sumner and Stewart, 1992). Such rainfall-induced crusts typically present a more compact, less macroporous structure with a higher mechanical impedance and hydraulic resistance than the unaffected soil. Crusts may form in place as a direct consequence of wetting or drop impact (*structural* crusts) or as a result of deposition of eroded material (*depositional* crusts). In the latter case, the selectivity of sedimentation regarding particle size frequently results in a layered crust (Chen et al., 1980; Mualem et al., 1990; West et al., 1992).

Although the classification of surface crusts into structural or depositional crusts has been applied to coarse-textured soils (Chen et al., 1980; Tarchitzky et al., 1984), detailed observations led Valentin and Bresson (1992) to propose a more elaborate, genetic approach to the taxonomy of crusts in these soils. According to this proposal, structural crusts develop on newly exposed surfaces. They are characterized by a thin clayey band a few tenths of a millimeter thick covered by several millimeters of sorted sand depleted in silt and clay (Valentin, 1986). *Erosion* crusts form through erosion of the sand layer of structural crusts, following runoff initiation. *Runoff* crusts are believed to result from deposition under turbulent-flow conditions of material eroded from upslope, whereas sedimentation under laminar-flow conditions leads to the formation of depositional crusts (Mücher and de Ploey, 1977; van der Watt and Valentin, 1992). For the latter two crust types, deposition occurs on top of the initial structural crust. All four crust types in Valentin and Bresson's (1992) model are part of a spatial and temporal continuum, which allows for the existence of genetic intergrades.

Independent of the model used and with the exception of the structural crust, the above definitions imply that the surface topography is an essential factor contributing to crust development. Erosion crusts should be more typical of upper topographic positions, whereas depositional and runoff crusts should occur preferentially in depressions. However, descriptions of the topographical location of crust samples are seldom provided (Rawitz et al., 1986; Ben-Hur et al., 1987; West et al., 1990; Radcliffe et al., 1991), and crust identification is usually based solely on morphological evidence. Hence many different interpretations have been given for crusts with seemingly identical morphologies, such as Tarchitzky et al.'s (1984) depositional crust, Arshad and Mermut's (1988) disruptional crust, or Valentin and Bresson's (1992) erosion crust. Information on the topographical position of crust samples should, in principle, dissipate some of the controversy concerning the genesis of particular crust morphologies.

Falayi and Bouma (1975), Mücher and de Ploey (1977), Valentin (1991), and Valentin and Bresson (1992) refer to the topographical position of the field crust samples they studied. However, none of these researchers

C.L. Bielders, ICRISAT Sahelian Center, B.P. 12404, Niamey, Niger (via Paris); P. Baveye, Dep. of Soil, Crop, and Atmospheric Sciences, Cornell Univ., Ithaca, NY 14853; L.P. Wilding and L.R. Drees, Dep. of Soil and Crop Sciences, Texas A&M Univ., College Station, TX 77843; and C. Valentin, ORSTOM, B.P. 11416, Niamey, Niger. Received 23 May 1994. *Corresponding author (pcb2@cornell.edu).

Published in Soil Sci. Soc. Am. J. 60:843-855 (1996).

Abbreviations: PPL, plane polarized light; B&W, black and white; BSE, backscattered electron; SEM, scanning electron microscope; SEI, scanning electron image; CL, crust layer; RDP, related distribution pattern; M-D, micromass-depleted; C/WI, compacted/washed-in.

actually describe the spatial distribution of crusts. Except at the centimeter or millimeter scales that are easily accessible through thin sections (Arshad and Mermut, 1988; Levy et al., 1988; Bresson and Boiffin, 1990; Gimenez et al., 1992), the spatial distribution of crusts is also generally ignored in laboratory experiments.

In this study, we investigated the spatial dependence of crust morphology on tillage-induced microrelief in a coarse-textured Ultisol from southern Togo. A primary objective of the research was to analyze combined micromorphological and topographic information to identify the mechanisms of crust formation. A second objective was to use the same data to evaluate the validity of a number of recent conceptual crust genesis models (Mualem et al., 1990; Valentin and Bresson, 1992; West et al., 1992).

MATERIALS AND METHODS

Field experiments were conducted on the research station of the Institut National des Sols at Glidji (Aneho), in the terres de Barre region of south eastern Togo (West Africa). The soils of the plateaus in this region are classified as fine-loamy, siliceous, isohyperthermic, Paleustults (Soil Survey Staff, 1992). The main physical and chemical characteristics of the A horizon of the experimental plot are as follows: thickness = 25 to 30 cm, sandy texture (4%, <2 μm; 5%, 2–50 μm; 15%, 50–100 μm; 64%, 100–500 μm; 12%, 500–2000 μm) (pipette method; Gee and Bauder, 1986), bulk density = 1.5 Mg m^{-3} (150 10^{-6} m^3 core; Blake and Hartge, 1986), organic C = 0.24 g kg^{-1} (loss on ignition; Nelson and Sommers, 1982), saturated hydraulic conductivity = 2 10^{-4} m s^{-1} (constant head method on undisturbed cores 70 mm in diameter and 100 mm long; Klute and Dirksen, 1986), pH = 6.1, cation-exchange capacity = 2.6 $cmol_c$ kg^{-1} (NH_4OAc at pH 7; Rhoades, 1982), exchangeable sodium percentage = 0.4% (NH_4OAc at pH 7; Rhoades, 1982). The clay fraction is dominated by kaolinite and hematite (x-ray diffraction, porous ceramic plate method; Whittig and Allardige, 1986). The soils at Glidji are described as strongly degraded by Poss et al. (1990).

At the beginning of the main rainy season in April 1992, a 10 by 10 m area was hoed manually to a depth of 0.10 to 0.15 m and raked to remove large organic debris. It had been continuously cultivated by hand since 1981 with a maize (*Zea mays* L.) and cassava (*Manihot esculenta* Crantz) rotation. Within this area, duplicate 1-m^2 runoff plots located 3 m apart (center-to-center) were delimited on the same day by means of a steel frame pushed into the soil to an approximate depth of 50 mm. The mean slope of both plots was 0.02 m m^{-1}. The frame was perforated on the downslope end to permit runoff collection (Asseline and Valentin, 1978). Runoff Plots A and B were exposed to natural rainfall for 44 and 47 d, respectively. Total rainfall and runoff were checked daily. Rainfall intensities were recorded automatically at 60-s intervals with a rainfall gauge. Data for some rainfall events were not available due to defective equipment.

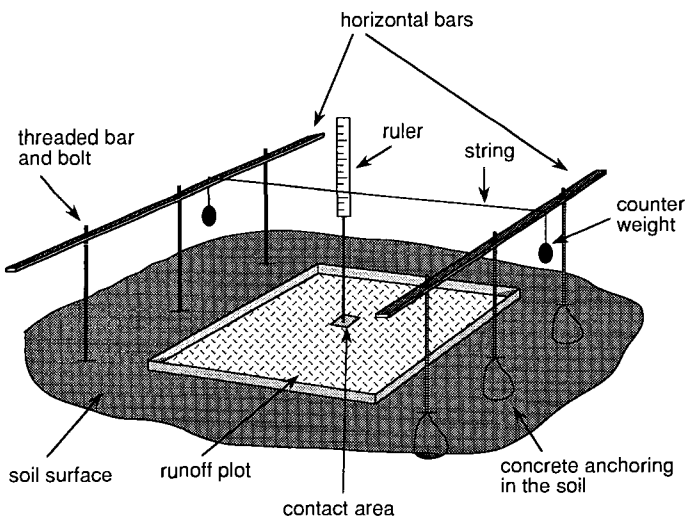

Fig. 1. Setup used for measuring the surface topography of 1-m^2 plots.

The topography of the runoff plots was monitored three times; 1, 9, and 43 d after tillage for Plot A and 1, 12, and 43 d after tillage for Plot B. It was measured on a 0.05-m grid with the equipment described in Fig. 1. Two horizontal bars created a permanent horizontal reference plane. A strip of millimeter-ruled paper affixed to a rod ended by a 1 × 10^{-4} m^2 (1 cm^2) contact area was used as a ruler. The runoff plots were manually scanned with the ruler, and the height variations were recorded. The lightweight ruler did not result in any visible soil disturbance on crusted surfaces. However, the first measurement was made immediately after the first rainfall event because the extremely weak coherence of the tilled dry soil could not sustain the ruler's weight. Measurements were reproducible to within ±1 mm. Points along the edge of the frame were not measured because of edge effects.

Two mapping units were defined within the runoff plots based on the color of the soil surface. Light areas (L) corresponded to zones covered predominantly by sand-sized quartz grains, whereas darker areas (D) were dominated by finer-textured material. The boundaries between mapping units were drawn by hand with a 0.1-m grid superimposed on the runoff plot for reference.

Before crust sampling, the runoff plots were exposed to a simulated rainfall of 60 mm h^{-1} for 1 h using a simulator modified from Asseline and Valentin (1978). Final infiltration rates were calculated by difference between the simulated rainfall intensity and final runoff rate. Approximately 1 h after the simulated rainfall, a total of 24 samples were taken along linear transects (Plot A, 3 transects and 16 samples; Plot B, 2 transects and 8 samples). Aluminum boxes 70 mm long by 40 mm wide by 40 mm high were used for sampling undisturbed crusts. All crust samples were air dried and impregnated under vacuum with a polyester resin (Castolite, Buelher Inc.). Two to six 60 by 40 by 30 μm vertically oriented thin sections were cut out of each sample. The procedures used followed those described by Jongerius and Heintzberger (1975). Some thin sections were machine ground to a thickness of ≈ 100 μm to allow better visualization of optical density changes within the crust. Six control samples of the freshly hoed soil taken just outside the runoff plots were sampled with great care and treated similarly. All thin sections were described according to the general guidelines provided by Bullock et al. (1985).

Black and white, 5× magnified images were obtained from direct projections of the ~ 100-μm thick sections onto photographic paper by means of a photographic enlarger (Gavasci and Eastler, 1972). The photographs were scanned with a flat-bed scanner (Abaton Scan 300/GS) at a resolution of 300 dots per inch. The digital images (16.9 μm/pixel resolution) were analyzed with the public domain NIH-Image 1.49 software[1]) to derive distribution profiles for pores and opaque material after segmenting the images at two cutoff values (pore–quartz grain and quartz grain–opaque material). General information concerning the concepts and terminology of image

processing and analysis can be found in Russ (1992) and Moran et al. (1989). The contrast between pores >100 μm in diameter and quartz grains in images obtained from machine-ground thin sections was judged sufficient to allow for a good separation of these two components by segmentation, as judged from a visual comparison between the thresholded image and the thin section. The range of grey levels from pores <100 μm in diameter and from grains strongly overlapped. The separation of small pores from grains by segmentation was therefore not attempted, and only pores >100 μm in diameter were considered in the determination of porosity profiles or pore size distributions. For opaque material, the threshold value was chosen arbitrarily based on the grey level of the lightest area that could be identified as micromass from a visual comparison between the thin section and the digital B&W image. Care was taken not to include grain edges in significant amounts. Only accumulations >10 pixels in area were considered for micromass profiles because it was not possible to establish a unique correspondence between areas <10 pixels in the digital image and micromass accumulations in the thin section. The threshold values were estimated by eye independently for each image by a single operator. Areal density is defined as the ratio of the area (number of pixels) occupied by a particular fabric unit to the total analyzed area (total number of pixels). In the case of distribution profiles, areal densities are calculated for fixed depth increments.

To reduce the microvariability in porosity and micromass profiles, the areal densities were averaged across 200 μm depth increments. The micromass and porosity profiles were further averaged across six 35-mm-high by 4-mm-wide digitized sections of the B&W image from a single thin section. Because of the variable thickness of the M-D layer, the profiles were centered on the clay band. In other words, the latter was taken as the depth reference, not the soil surface. The average thickness of the M-D layer was determined on B&W photographs by measuring the entire area of the M-D layer and dividing that area by the width of the thin section on the photograph.

Forty-two 4 by 3 mm BSE images (30× magnification, 30 kV) were obtained from two C-coated thin sections of crusts taken from two different plots and presenting a well-developed C/WI layer. The sections had been polished sequentially with grinding powders of 27-, 9-, 3-, and 1-μm grain size. The images were taken along two horizontal transects: one immediately below the clay band and one ≈20 mm below the surface in the layer unaffected by crusting. The digital images were processed by means of the NIH-Image software. The areal densities of skeleton grains (all grains >20 μm in diameter with a BSE signal intensity stronger than or equal to the signal from quartz) and micromass (material with a BSE signal intensity weaker than quartz as well as all grains <20 μm in diameter) were measured with the same threshold values for all images. Image resolution was 3.9 μm/pixel. The relatively simple procedure used for image processing and analysis is described in Bielders (1994). Autocorrelation analysis revealed that there was no spatial autocorrelation between images from a given transect. The statistical significance of the difference in areal density values between two layers of the same kind was tested with an independent *t*-test. The difference between the C/WI layer and the unaffected layer of each crust sample was tested with both independent and paired *t*-tests. Both analyses lead to the same conclusions, indicating the absence of pairing between images from different layers.

[1] Wayne Rasband, NIH Image: An image processing software package for the Macintosh II. Available free of charge via the Internet by anonymous ftp from zippy.nimh.nih.gov or from Library 9 of the MacApp forum on Compuserve.

RESULTS AND DISCUSSION

Of the 217 mm of rainfall that fell between the time of runoff plot preparation and crust sampling, 38 and 32 mm were collected as runoff from Plots A and B, respectively, corresponding to average runoff coefficients of 17 and 15%. The final infiltration rate following the 1-h simulated rainfall was 28 and 30 mm h^{-1} for Plots A and B, respectively. The corresponding runoff coefficients were 28 and 23%, respectively. These numbers emphasized the similar hydrological properties of Runoff Plots A and B. No distinction was therefore made between crust samples taken from either plot.

Crust Micromorphology

A comparison of the reference uncrusted samples and the samples collected after exposure to natural rainfall revealed a strong restructuring of particles at the soil surface following drop impact. The various crusts observed in the thin sections could be represented by two types (Types 1 and 2) and by morphological intergrades.

Soil Initial State and Material Underlying the Crusts

The material underlying the surface crust was considered to be *unaffected material*; i.e., there was no visual evidence of disturbance by drop impact or surface-water flow, nor any indication that it had been enriched or depleted by eluviation or illuviation. Since the micromorphology of the reference samples closely resembled that of the unaffected material, a separate description is not provided. The unaffected layer was similar for all crust types. It consisted mostly of loose, apedal material composed dominantly of unsorted quartz grains. Coarse-silt to fine-sand, redish-brown fabric units (most likely Fe oxides) with a speckled-striated birefringence fabric were homogeneously distributed throughout the groundmass. The coarse/fine RDP with a threshold at 20 μm ($c/f_{20\mu m}$) was mostly chitonic, the coatings being 5 to 25 μm thick. Additional micromass was present either as bridges (gefuric RDP) or inside intergranular pores (enaulic RDP). Under PPL and at magnifications >200×, the micromass appeared granular. The porosity of the apedal material included simple and complex packing voids between loosely packed grains. In many thin sections, small 1-mm- to 1-cm-diameter aggregates were observed. They generally did not occupy more than 5 to 15% of the thin section area by visual estimation.

Type 1 Crust

Two main layers were observed in Type 1 crusts (Fig. 2a): (i) CL 1: This M-D layer was composed dominantly of sand-sized quartz grains and was <12 mm thick, its thickness increasing downslope. Below a depth of 0.5 to 1 mm, fine sand-sized to coarse silt-sized redish-brown fabric units identical to those described in the unaffected layer were observed. Coatings and bridges were absent. Pores were essentially simple packing voids and vesicles,

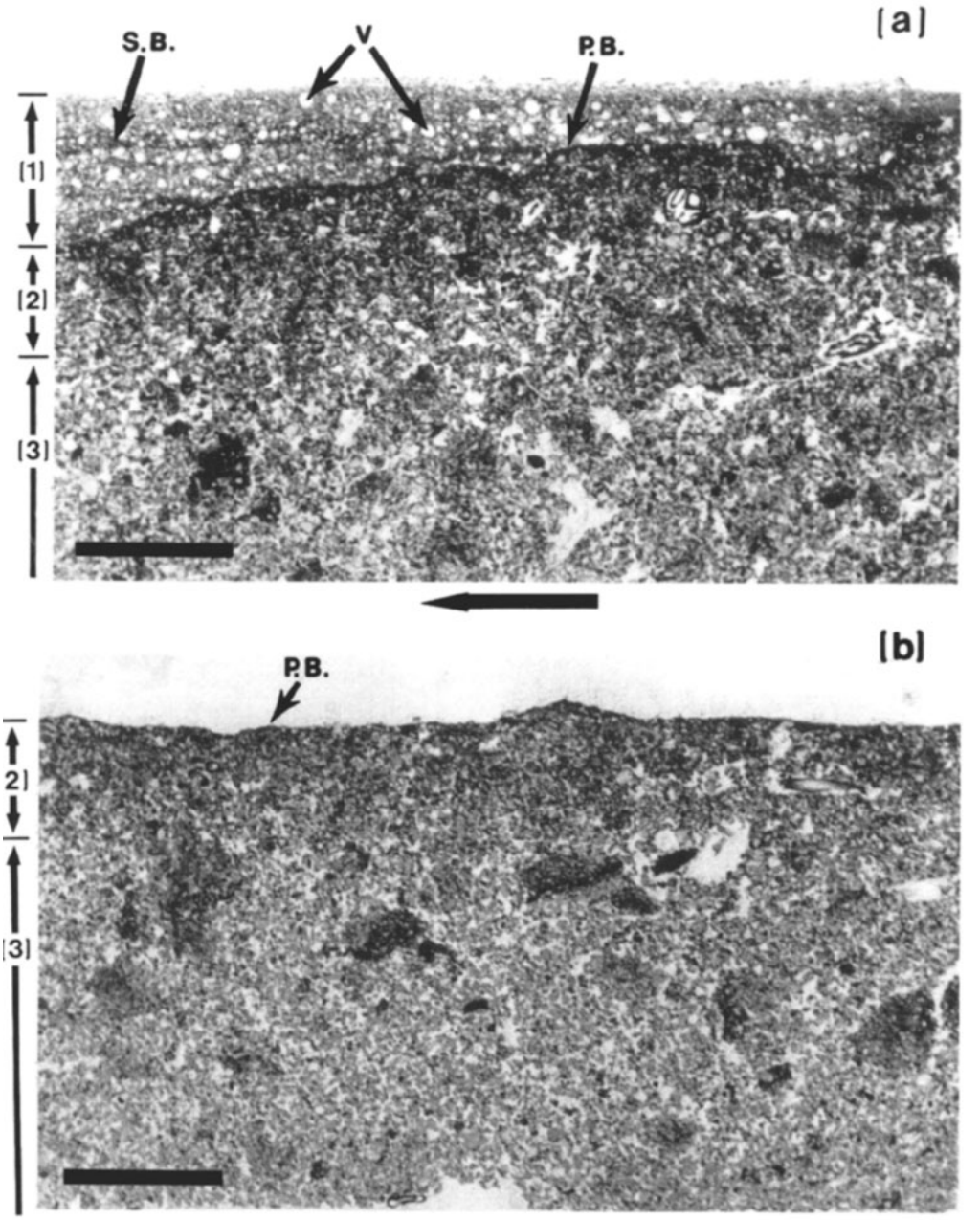

Fig. 2. Photographs of 100-μm-thick sections of observed crust types. (a) Type 1 crust, (b) Type 2 crust. (1) Crust Layer 1, (2) Crust Layer 2, (3) unaffected material. P.B. = primary clay band, S.B. = secondary clay band, V = vesicle. Arrow points downslope. Bar = 10 mm.

the latter ranging in diameter from 0.2 to 1 mm, with a mean of 0.35 mm. The vesicles never extended into the underlying CL 2 and could readily be identified in the field during sampling. (ii) CL 2: The boundary between CL 1 and CL 2 was sharp but undulating (Fig. 2a). Two sublayers could be defined based on their RDP. The uppermost sublayer had a close porphyric $c/f_{50\mu m}$ RDP at magnifications <200× (Fig. 3a). It will hereafter be referred to as the *primary clay band*, although it was actually enriched in all forms of micromass. The micromass appeared granular with no particular orientation (Fig. 3b). The lower boundary of the clay band extended irregularly into the pores of the underlying material (Fig. 3a). Hence the thickness of the clay band varied considerably, from 150 to 500 μm. *Secondary clay bands* were observed above the primary clay band whenever the thickness of the overlying M-D layer exceeded ~5 mm. In general, only the primary clay band was continuous across a given thin section.

Below the primary clay band was a region with a dominantly enaulic $c/f_{50\mu m}$ RDP. Additional micromass was present as partial coatings and bridges between grains. The areal density of both grains and micromass appeared higher than in the unaffected material. This C/WI layer was up to 10 mm thick. The boundary with the unaffected material was diffuse.

Vertical changes in porosity and micromass areal density are shown in Fig. 4 for a Type 1 crust, confirming the previous visual observations. The position of the upper dashed line in Fig. 4 corresponds to the depth of

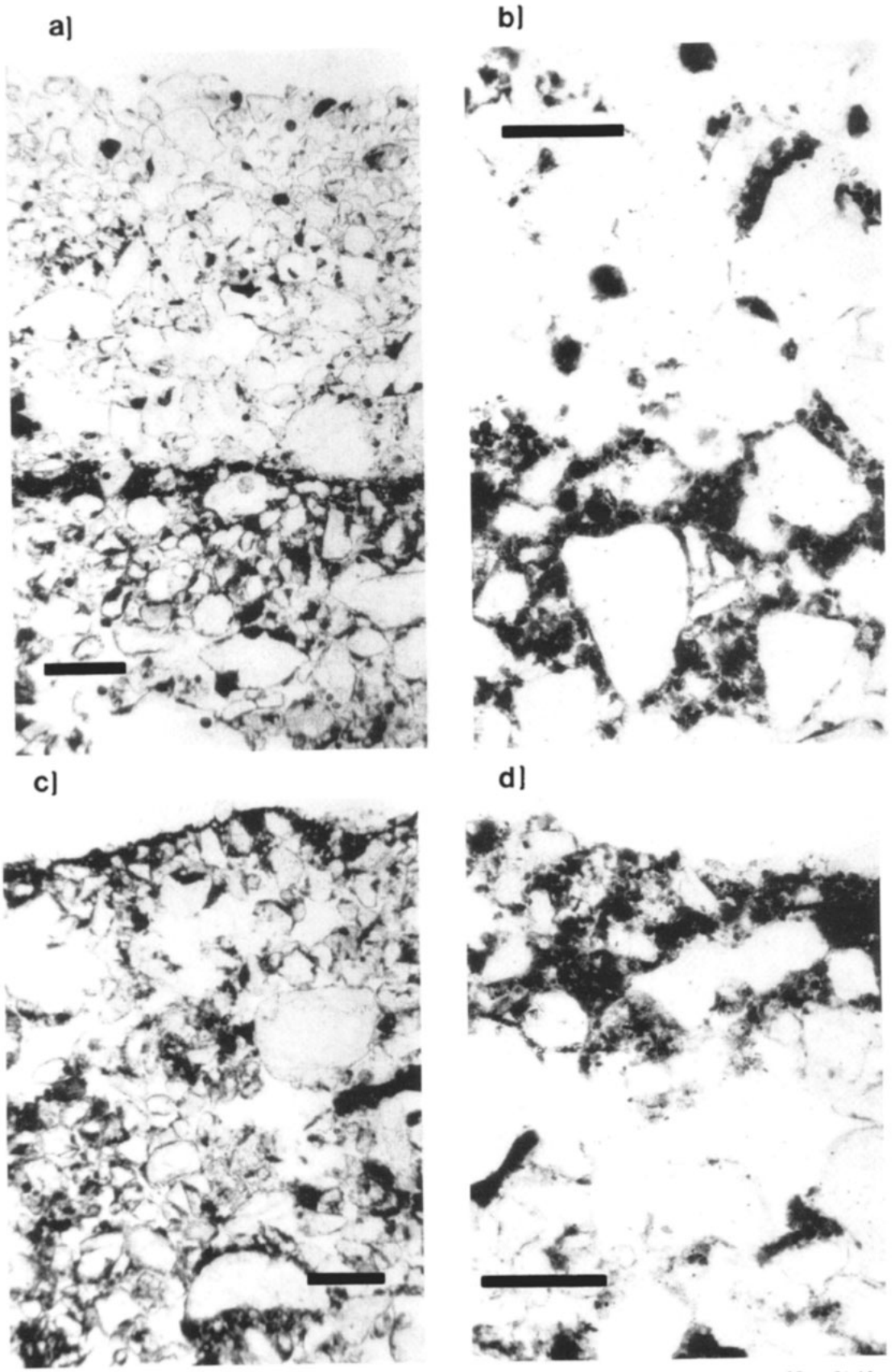

Fig. 3. Plane polarized light photographs of clay band for two crust types at two magnifications. (a) Type 1 crust 25×. (b) idem, 100×. (c) Type 2 crust, 25×. (d) idem, 100×. (a) and (c) are from 100-μm thick section; (b) and (d) are from 30-μm thin section. Bar: 25× = 0.5 mm, 100× = 0.1 mm.

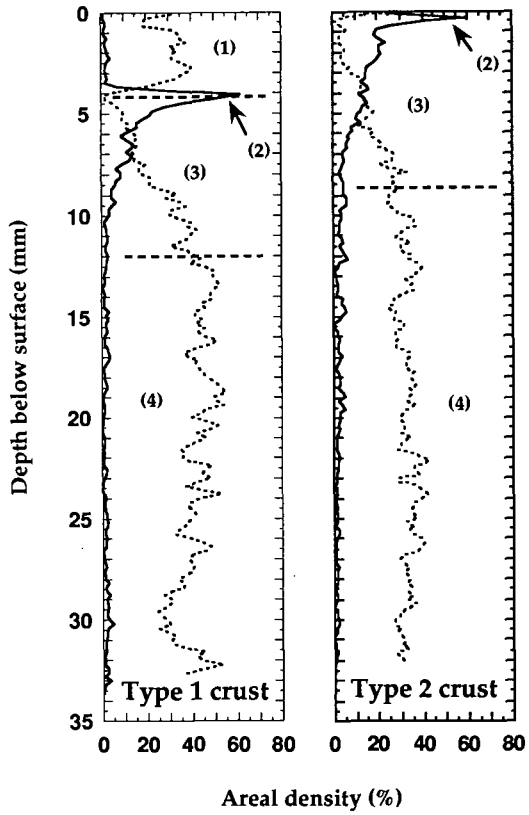

Fig. 4. Porosity profiles (dotted line) and micromass areal density profiles (solid line) for Type 1 and Type 2 crusts. Horizontal dashed lines mark approximate boundaries between layers. (1) micromass-depleted layer, (2) clay band, (3) compacted/washed-in layer, (4) unaffected material.

the clay band. Since the transition between the C/WI layer and the unaffected material is gradual, the lower dashed line in Fig. 4 is only indicative of the approximate location of the boundary between these two layers. From the areal density values in the M-D layer (Zone 1), the depletion in micromass compared with the unaffected layer is not evident. This is because the redish-brown fabric units occurring in this layer are opaque. They were therefore classified as micromass. A rapid drop to virtually 0% porosity and a sharp rise in micromass areal density mark the upper limit of the clay band. The C/WI layer (Zone 3) is 6 to 8 mm thick with a gradual increase in porosity and a decrease in micromass areal density with depth. Below ~12-mm depth, unaffected material with very low areal micromass densities is found (Zone 4).

Type 2 Crust

Type 2 crusts were limited to a CL 2 (Fig. 2b). Sand material above the clay band was absent or limited to a single, noncontinuous layer of grains often partially embedded in the clay band (Fig. 3c). Both the thickness (100–500 μm) and granular appearance of the clay band (Fig. 3d) were comparable with the primary clay band of the Type 1 crust. A C/WI layer reached to a maximum depth of 10 mm. The porosity and micromass areal density profiles again support these observations (Fig. 4). The average porosity of the unaffected layer is ≈ 10% less in the Type 2 crust than in the Type 1 crust. This could be related to differences in the initial soil bulk density following tillage.

Crusts of Type 1 and 2 represent morphological extremes. Most observed crusts in any given thin section had an intermediate morphology (Fig. 5); i.e., the primary clay band was always present but the thickness of the M-D layer varied. Since the thin sections were ~60 mm wide, the crust in each thin section usually covered a certain range in morphologies, the thickness of the M-D layer varied, the clay band could be exposed on one end and not the other, etc. This variability is apparent in the distribution of the number of samples (Fig. 5). Some degree of compaction/washing-in was observed in 11 out of 24 samples, but its occurrence was unrelated to any one crust type. It appears that the C/WI layer is

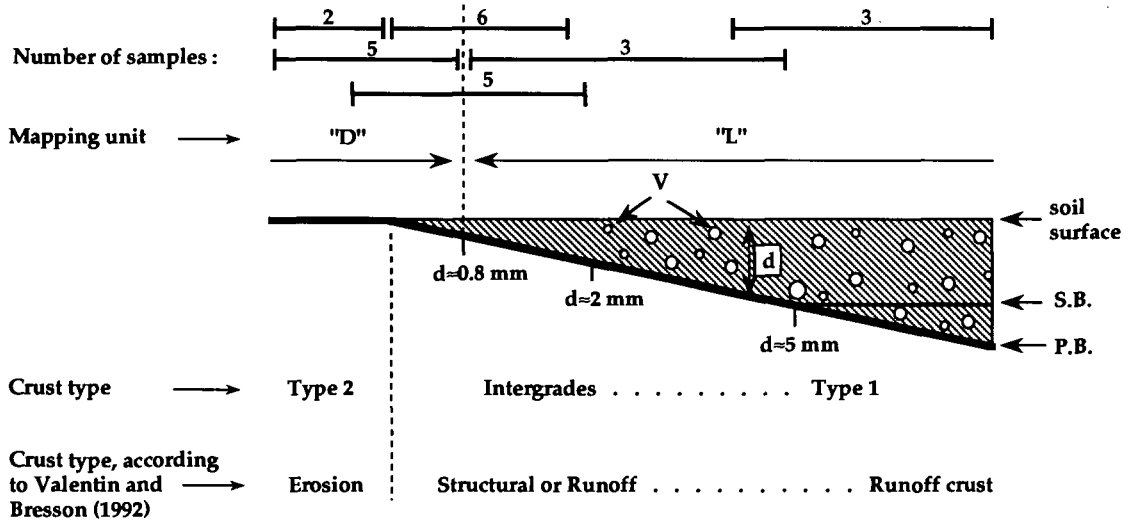

Fig. 5. The range of crust mophologies observed in the thin sections. The hatched area represents the micromass-depleted layer. V = vesicle, P.B. = primary clay band, S.B. = secondary clay band. Mapping Unit D corresponds to dark-colored surfaces (i.e., finer-textured), whereas L corresponds to light-colored surfaces (coarse-textured). The numbers at the top refer to the number of crust samples within each category.

a spatially variable feature of field crusts. Some of this variability is readily apparent in Fig. 2a and 2b.

In the literature, layers with characteristics similar to the C/WI layer are often simply referred to as *washed-in layers* (West et al., 1992). However, an increase in micromass areal density may in principle result from compaction as well as washing-in. To evaluate the relative importance of these two processes, BSE SEM images were used to quantify the areal density of both skeleton grains and micromass in C/WI and unaffected layers. From these measured values, areal porosities and micromass-to-grain ratios were calculated (Table 1). An increase in grain areal density between the unaffected and the C/WI layer could indicate compaction since washing-in probably does not affect the coarse fraction of the soil. An indicator of washing-in would be an increased micromass to grain ratio. For the two chosen crust samples with well-developed C/WI layers corresponding to Fig. 2a and 2b, the areal grain density and micromass-to-grain ratios were significantly higher in the C/WI layer than in the unaffected material (Table 1). This suggests that both compaction and washing-in contributed to the development of the C/WI layer. If one assumes that the micromass-to-grain ratio remains unaffected by compaction, 8 of the 13% decrease in porosity between the unaffected and C/WI layer in Sample 1 may be attributed to compaction (Appendix 1). The remaining 5% would then have been caused by the washing-in process. On the same grounds, compaction and washing-in processes contributed, respectively, 1 and 5% to the 6% increase in micromass in the C/WI layer. For Sample 2, 13 and 3% of the 16% porosity decrease in the C/WI layer may be attributed to compaction and washing-in, respectively, whereas each individual process contributed 3% to the 6% micromass increase.

Spatial Distribution of Crust Types

On Day 1 (Fig. 6a and 6c), the surface microrelief was very similar to the initial topography since the plots had only been exposed to one 5-mm rainfall of low maximum intensity (Fig. 7). The major axes of surface drainage are drawn in Fig. 6b and 6d, on the basis of the topography and of visual observations made during the simulated rainfall event. A map of the surface color of the runoff plots at the time of crust sampling is superimposed on all contour plots. Mapping units L and D correspond to light- and dark-colored areas, respectively.

The surface color and the corresponding surface texture of the mapping units were consistent with the morphology of the dominant crust type found within each unit. Of eight crust samples falling within the boundaries of Mapping Unit D, seven had a M-D sand layer <0.7 mm thick and their morphology resembled that of crust Type 2. A dark surface color is indeed expected from an exposed, or minimally covered, clay band. Of six samples located within Mapping Unit L, all had a M-D sand layer >0.8 mm. Their morphology could be associated with Type 1 crusts or with intergrades between Type 1 and 2, which have a well-defined M-D layer. The remaining 10 samples overlapped the mapping unit boundaries and were of Type 1 or transitional morphology (Fig. 5). This is in part because the transition between mapping units was continuous in the field and mapping unit boundaries could be drawn with an accuracy of ±25 mm at best. Since a correspondence between mapping unit and M-D layer thickness is observed, the surface color maps may be used as reasonable approximations of the spatial distribution of two classes of crusts: Type 2 crusts with an exposed or minimally buried clay band (Mapping Unit D), and Type 1 or intergrade crusts with a sufficiently thick M-D layer (Mapping Unit L).

Another general correspondence, between mapping units and initial topography, can be observed from Fig. 6a and 6c. In particular, Mapping Unit D encloses most of the higher elevation points. This correspondence is weaker at the time of sampling (Fig. 6b and 6d). Mapping Unit L is generally associated with depressions, downslope areas, and major drainage axes. It is also found on extended gentle slopes of topographic highs (Zone 1 in Fig. 6b, Zone 6 in Fig. 6d). Mapping Unit D still encloses most of the higher points of the relief as well as the upper parts of slopes. Most striking, however, are the D units of Zones 2 and 3 in Fig. 6b and Zones 4 and 5 in Fig. 6d, which are associated with upper topographic positions only on the initial topography.

New contour maps were created by subtracting the topography on Day 9 (t2, Plot A) or Day 12 (t2, Plot B) from the final topography on Day 43 (t3; Fig. 6e and 6f). Positive values indicate a net lowering of the surface with time, which can be due to both soil settling and erosion. On the contrary, height increases can only reflect deposition. A comparison of Fig. 6a through 6e and 6c through 6f reveals that the areas of highest elevation in the initial topography were also the areas that showed a maximum decrease in altitude with time. Concomitantly, Fig. 6e and 6f indicate that Mapping Unit L contains virtually all areas where deposition is certain to have occurred (height increases >2 mm), as well as some areas that show only minimal height variations (height changes from −2 to 2 mm). Mapping Unit D encloses most areas where height decreased by more than 2 mm during the t2-t3 period (Fig. 6e and 6f). Such a dependence of the spatial distribution of the mapping units, and hence of the M-D layer thickness, on the initial

Table 1. Areal density of grains and micromass as measured from backscattered electron images of the compacted/washed-in (C/WI) layer and unaffected layer of two crust samples and calculated areal density of pores and micromass to grain ratio (mean ± standard deviation).

	Crust Sample 1		Crust Sample 2	
Areal densities of	C/WI layer n† = 12	Unaffected n = 12	C/WI layer n = 9	Unaffected n = 9
	%			
Grains (1)	45 ± 3 a‡	38 ± 5 b	50 ± 3 c	40 ± 5 b
Micromass (2)	14 ± 1 a	8 ± 2 b	15 ± 1 c	9 ± 1 b
Pores = 100 − (1) − (2)	41 ± 3 a	54 ± 5 b	35 ± 3 c	51 ± 6 b
Micromass/grain = (2)/(1)	31 ± 3 a	21 ± 5 b	30 ± 3 a	23 ± 2 b

† n = number of images analyzed in each layer.
‡ Values of the same variable followed by the same letter are not significantly different between layers (P = 0.05).

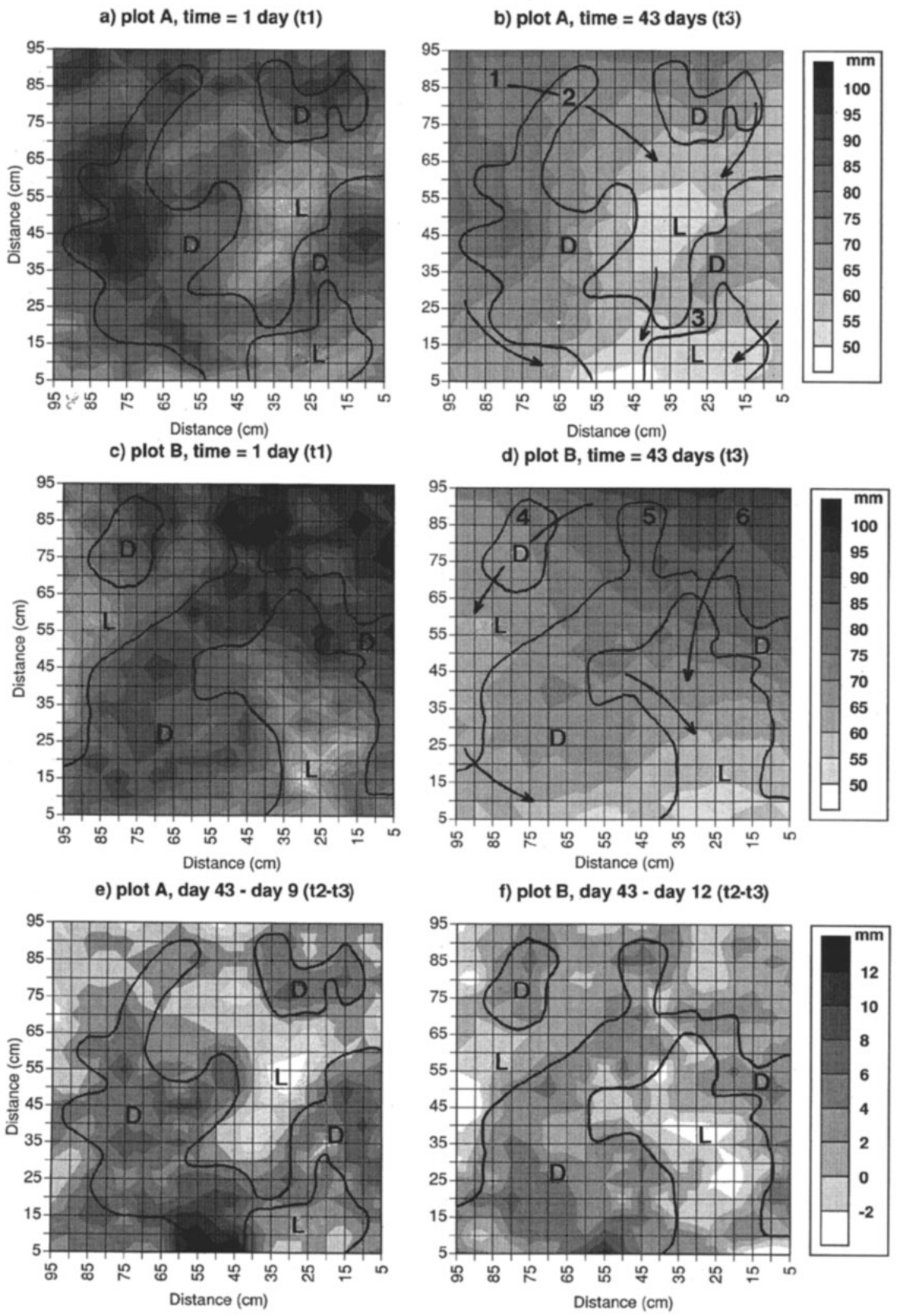

Fig. 6. Contour plots of the initial and final surface topography of Runoff Plots A and B, and difference between the topography at Day 9 (Plot A) or Day 12 (Plot B) and the final topography at Day 43. D and L are two surface color mapping units (see text). Zones 1 to 6 are discussed separately in the text.

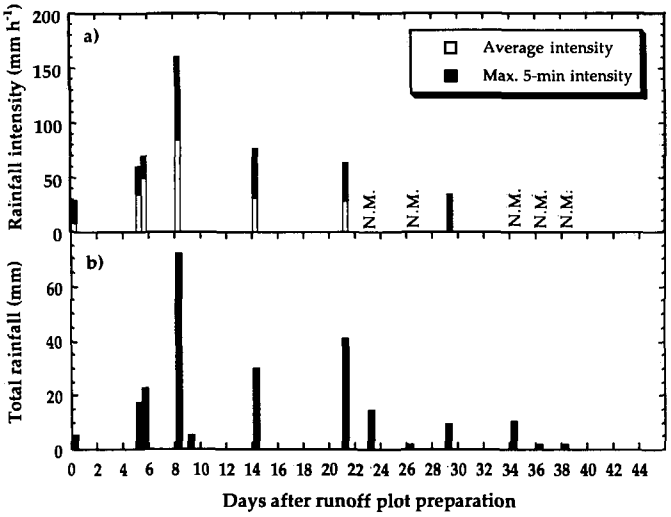

Fig. 7. Rainfall distribution and characteristics during the period of crust development. (a) Average rainfall intensity and maximum intensity during a 5-min period; (b) Total rainfall (NM = not measured).

topography suggests that erosion and deposition processes largely governed crust development.

Exposed clay bands have often been attributed to deposition of fine material from turbid water at the end of rainfall events (Norton, 1987; Mualem et al., 1990; West et al., 1992). In this study, however, Type 2 crusts were found predominantly on upper topographic positions and such areas were at best exposed to a runoff water layer a fraction of a millimeter thick. On the other hand, clay accumulation was never observed at the soil surface in depressions. It seems improbable that a band of micromass 100 to 500 μm thick could deposit on topographic highs from a microscopic film of running water whereas it did not form in depressions where the depth of ponding was observed to reach up to 15 mm. Arshad and Mermut (1988) described a band-like layer – the disruptional seal – whose morphology was attributed to coalescence and compaction of aggregates. In the present case, this hypothesis is not very satisfactory either because of the very low clay content and weak aggregation of soils at Glidji. For the same reasons, compaction of the soil surface (McIntyre, 1958; Bresson and Boiffin, 1990) is also an unlikely explanation for clay band formation in these coarse-textured soils.

According to Valentin and Bresson (1992), a structural crust may evolve into an erosion crust when its washed-out layer is eroded by splash and runoff. Erosion crusts should therefore be associated with potentially erodable topographical positions, and they should consist solely of an exposed clay band. Since Mapping Unit D coincides with areas that had most likely been subject to erosion (Fig. 6e and 6f), it appears that Type 2 crusts may correspond to erosion crusts. This conclusion also agrees with the morphological description of Type 2 crusts.

Valentin and Bresson's (1992) model can be further tested against the spatial distribution of Type 1 crusts. Since it was shown to encompass all crusts with a M-D layer >0.8 mm, Mapping Unit L should include Type 1 crusts and hence the depressional areas where deposition occurred. This is indeed observed (Fig. 6e and 6f). However, in contrast with Mapping Unit D, which covers a narrow range of possible crust morphologies, Mapping Unit L can include both well-developed runoff crusts and structural crusts as a result of its definition. Mapping Unit L may also comprise intergrades between structural crusts and erosion crusts or between erosion crusts and runoff crusts, as long as the M-D layer thickness exceeds a certain minimum value to ensure a light surface color. The fact that Mapping Unit L encloses areas other than depressions does therefore not invalidate Valentin and Bresson's (1992) model.

According to Valentin and Bresson (1992), the presence of a clay band should be a spatially continuous feature. Methodologically, given the size of the thin sections used in this study, it is not possible to show explicitly that the clay band is continuous across distances >0.1 m. Nevertheless, millimeter-, centimeter-, and decimeter-scale observations of crust morphologies point to such a continuity. At the millimeter scale, crust samples with a transitional morphology between Type 1 and Type 2 crusts clearly reveal the continuity of the clay band (Fig. 8a). The M-D layer thickness is observed to increase downslope, as would be expected if deposition contributed to its formation. At larger length scales, the continuity of the clay band is also apparent (Fig. 8b). Occasionally, millimetric depressions, about 5 mm wide and 0.5 to 1 mm deep, were found in the clay band of Type 2 crusts. These depressions sometimes had a M-D layer (Fig. 8b). Other examples of such small-scale transitions can be seen on the left side of Fig. 8a. In spite of these small depressions, the microstructure of the clay band appears remarkaby uniform in all available thin sections. This observation, along with the continuity of the clay band, strongly suggests that a single process was responsible for the development of the band across the microlandscape.

Because of the inferred dependence of crust formation on erosion, transport, and deposition processes, one expects the spatial distribution of crusts to be complex but not intrinsically haphazard. Several factors probably affect the relative intensity of erosion vs. deposition at any given point on the microrelief as is the case for large-scale erosion. Among these factors are the slope angle, length, or curvature, the catchment area, or the time distribution of rainfall characteristics. However, whereas the topography remains virtually constant across significant periods of time for large length scales (e.g., >100 m), at the small scales discussed here, the microrelief rapidly evolves during the course of one or several rainfall events (Fig. 6). Small initial local highs or depressions may become part of a continuous slope with time (Fig. 9). At a later stage, the entire slope may be affected by erosion, as water and sediment flow conditions are altered. The succession of L and D mapping units around Zones 2 (Fig. 6b) and 4 (Fig. 6d) are believed to illustrate such cases. Their presence cannot easily be explained on the basis of the topography at the time of sampling. As the initial highs of Zones 2 and 4 were eroded and the surrounding depressions filled, a continuous slope

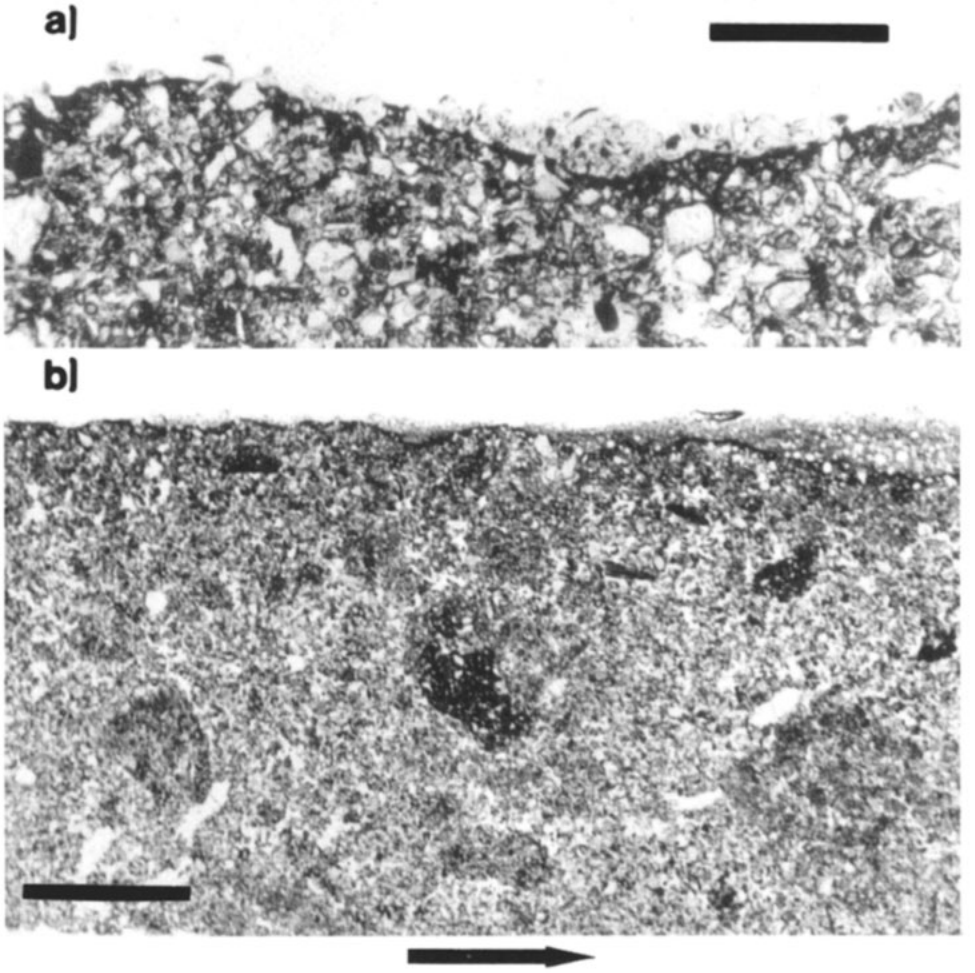

Fig. 8. Crust morphology transitions at two observation scales. (a) millimeter scale, bar = 2 mm, (b) decimeter scale. Bar = 10 mm. Arrow points downslope. Note the continuity of the clay band.

developed. The presence of erosion crusts in Zones 3 (Fig. 6b) and 5 (Fig. 6d) can be similarly explained. The process depicted in Fig. 9 leads to an areal extent of erosion crusts that progressively increases with time. In semi-arid rangelands of the West African Sahel where crusts are not disrupted by agricultural practices, the predominance of erosion crusts has been noted (C. Valentin, unpublished data). In agricultural systems, tillage interferes with crust development and a more even distribution of various crust types can be expected.

The presence of Mapping Unit L on upper topographic positions such as Zones 1 (Fig. 6b) and 6 (Fig. 6d) may be explained by the fact that both runoff and structural crusts fit within the definition of this mapping unit. These zones may be characterized by structural crusts rather than erosion crusts because the gentle slopes and the proximity to the edge of the runoff plot limited the erosion rate.

Depositional crusts were not observed in this study. Following the simulated rainfall, ponding of the depressional areas lasted less than ~20 min as a result of the relatively high final infiltration rate of the crusted soils. This is not long enough for significant particle sorting by sedimentation to occur. Also, the clay content of the runoff water may have been too low.

Since its description by McIntyre (1958), the term *washed-in layer* has been used in the literature to describe any layer within a crust that presents a higher micromass density than the unaffected material (West et al., 1992). In this general sense, the term would apply to the entire CL 2 described above, since the clay band probably originates from a washing-in process in the initial structural crust (Valentin, 1986). However, washing-in is usually taken to be synonymous to illuviation of dispersed clay (McIntyre, 1958; West et al., 1992). The appearance and anisotropic birefringence fabric of the micromass in the clay band is very similar to what is observed in the unaffected layer. In addition, the increased micromass density was noted mostly in the fraction that has an enaulic RDP, i.e., not in the form of coatings but rather as small aggregates of micromass. These observations may be more indicative of a sieving mechanism similar to that proposed by Valentin (1986) rather than illuviation of dispersed clay.

On morphological grounds, it appears that the permeability-limiting layers of runoff crusts are the clay bands,

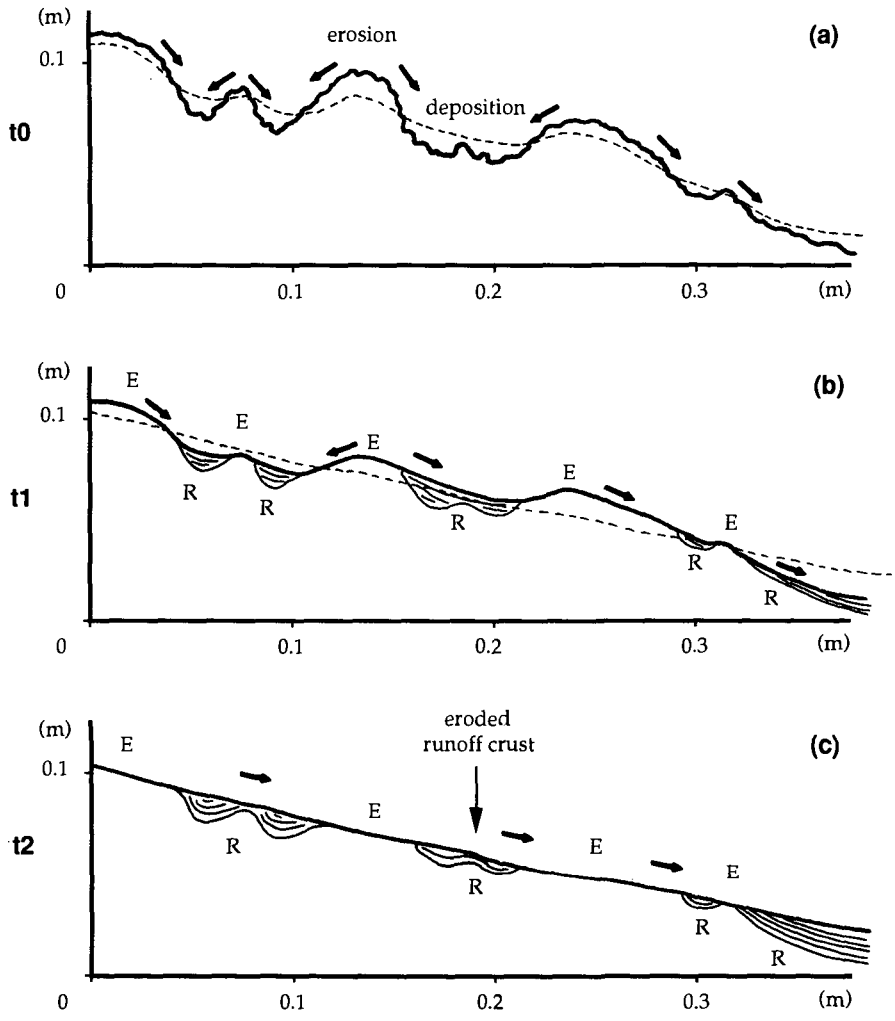

Fig. 9. Conceptual representation explaining the origin of sequences of runoff and erosion crusts along a continuous slope. R = runoff crust, E = erosion crust. Arrows indicate the dominant direction of transport of material.

in association with a C/WI layer whenever it is present. This is supported by the presence of vesicular pores in the M-D layer, which indicates reduced permeability below this layer. However, since vesicles contain entrapped air and therefore cannot conduct water, the M-D layer itself may actually contribute to the overall reduction of permeability of runoff crusts by decreasing the cross-sectional area of pore space available for flow. In further crust hydrodynamic studies on coarse-textured cultivated soils, we suggest that measurements should focus primarily on changes in crust permeability across distances >0.1 m, which is the smallest scale at which multiple clay bands in runoff crusts have been observed.

CONCLUSIONS

Aside from the clear demonstration that surface crusting does occur in coarse-textured Ultisols under field conditions and that it appears to have a significant impact on the hydrological properties of these soils, the key results of our research are relative to the influence of surface microrelief on the spatial distribution of crusts and to the mechanisms responsible for surface crusting.

The results illustrated in Fig. 6 show that to understand the spatial distribution of crusts at the time of sampling, one needs to consider the entire history of the surface microrelief since the onset of the field experiments, not merely the topography at the time of sampling. This requirement will undoubtedly complicate efforts to model mathematically the spatial distribution of surface crusts under field conditions.

The dependence of the spatial distribution of crusts on the initial plot microrelief suggests that erosion and deposition processes governed to a large extent the development of the crusts. This observation is in agreement with the crust genesis model of Valentin and Bresson (1992), as is the presence of a spatially continuous clay band observable across a range of scales from 0.01 to 0.1 m (Fig. 8). Other possible explanations proposed in the literature for the existence of such clay bands — invoking the deposition of fine material, the coalescence of aggregates, or the compaction of the soil surface — could not account adequately for our results. However, it is possible that these alternative mechanisms would be applicable under different conditions.

ACKNOWLEDGMENTS

This research was funded in part through the Title XII Collaborative Research Support Program Subgrant SM-CRSP-012 and through an Olin Fellowship awarded to one of us (C.L.B.) by Cornell's graduate school.

APPENDIX 1

Sample calculation for Crust Sample 1 (Table 1) of the respective contributions of compaction and illuviation to the porosity decrease and micromass increase between the unaffected layer and C/WI layer of surface crusts.

The basic assumptions are that (i) compaction leads to an increase in grain (G) and micromass areal densities (M), but that the micromass to grain ratio (M/G) remains unaffected; (ii) changes in grain areal density in the C/WI layer are only due to compaction and changes in the M/G ratio are entirely due to illuviation.

Increase in G due to compaction:

$$45 - 38 = 7\% \quad [1]$$

The total M that should be associated with the grains in the C/WI layer in the absence of illuviation is given by (G, C/WI layer) × (M/G, unaffected layer):

$$45\% \times 0.21 = 9\% \quad [2]$$

Increase in M due to compaction = [2] − [M, unaffected layer]:

$$9 - 8 = 1\% \quad [3]$$

Increase in M due to illuviation = [M, C/WI layer] − [2]: 14 − 9 = 5%

Contribution of compaction to the porosity decrease = [1] + [3]: 7 + 1 = 8%

Contribution of illuviation to the porosity decrease = [M, C/WI] − [2]: 14 − 9 = 5%

REFERENCES

Arshad, M.A., and A.R. Mermut. 1988. Micromorphological and physico-chemical characteristics of soil crust types in northwestern Alberta, Canada. Soil Sci. Soc. Am. J. 52:724–729.

Asseline, J., and C. Valentin. 1978. Construction et mise au point d'un infiltromètre à aspersion. Cah. ORSTOM, ser. Pedol. 15(4): 321–349.

Ben-Hur, M., I. Shainberg, and J. Morin. 1987. Variability of infiltration in a field with surface-sealed soil. Soil Sci. Soc. Am. J. 51: 1299–1302.

Bielders, C.L. 1994. Surface crusting: Mechanisms of formation, spatial distribution and effect on infiltration. A case study on coarse-textured soils from southern Togo. Unpublished Ph.D. diss. Cornell University, Ithaca, NY (University Microfilm International Diss. Abstr. 95-01278).

Blake, G.R., and K.H. Hartge. 1986. Bulk density. p. 363–376. *In* A. Klute (ed.) Methods of soil analysis. Part 1. 2nd ed. Agron. Monogr. 9. ASA and SSSA, Madison, WI.

Bresson, L., and J. Boiffin. 1990. Morphological characterization of soil crust development stages on an experimental field. Geoderma 47:301–325.

Bullock, P., N. Fedoroff, A. Jongerius, G. Stoops, and T. Tursina. 1985. Handbook for soil thin section description. Waine Research Publications, Wolverhampton, UK.

Casenave, A., and C. Valentin. 1992. A runoff capability classification system based on surface features criteria in semi-arid areas of West Africa. J. Hydrol. (Amsterdam) 130:231–249.

Chen, Y., J. Tarchitzky, J. Brouwer, J. Morin, and A. Banin. 1980. Scanning electron microscope observations on soil crusts and their formation. Soil Sci. 130:49–55.

Falayi, O., and J. Bouma. 1975. Relationships between the hydraulic conductance of surface crusts and soil management in a Typic Hapludalf. Soil Sci. Soc. Am. Proc. 39:957–963.

Gee, G.W., and J.W. Bauder. 1986. Particle-size analysis. p. 383–412. *In* A. Klute (ed.) Methods of soil analysis. Part 1. 2nd ed. Agron. Monogr. 9. ASA and SSSA, Madison, WI.

Gavasci, A.J., and T.E. Eastler. 1972. New apparatus and methodology for thin-section photography. Geol. Soc. Am. Bull. 83:2843–2851.

Gimenez, D., R. Miedema, L.A.A. Eppink, and D. Schoonderbeek. 1992. Surface sealing and hydraulic conductances under varying-intensity rains. Soil Sci. Soc. Am. J. 56:234–242.

Jongerius, A., and G. Heintzberger. 1975. Methods in soil micromorphology. A technique for the preparation of large thin sections. Soil Survey Papers No. 10. Soil Survey Inst., Wageningen, the Netherlands.

Klute, A., and C. Dirksen. 1986. Hydraulic conductivity and diffusivity: Laboratory methods. p. 687–732. *In* A. Klute (ed.) Methods of soil analysis. Part 1. 2nd ed. Agron. Monogr. 9. ASA and SSSA, Madison, WI.

Levy, G.J., P.R. Berliner, H.M. du Plessis, and H.v.H. van der Watt. 1988. Microtopographical characteristics of artificially formed crusts. Soil Sci. Soc. Am. J. 52:784–791.

McIntyre, D.S. 1958. Permeability measurements of soil crusts formed by raindrop impact. Soil Sci. 85:185–189.

Moran, C.J., A.B. McBratney, and A.J. Koppi. 1989. A rapid method for analysis of soil macropore structure. I. Specimen preparation and digital binary image production. Soil Sci. Soc. Am. J. 53: 921–928.

Mualem, Y., S. Assouline, and H. Rohdenburg. 1990. Rainfall induced soil seal. (A) A critical review of observations and models. Catena 17:185–203.

Mücher, H.J., and J. de Ploey. 1977. Experimental and micromorphological investigation of erosion and redeposition of loess by water. Earth Surf. Processes Landforms 2:117–124.

Nelson, D.W., and L.E. Sommers. 1982. Total carbon, organic carbon, and organic matter. p. 539–581. *In* A.L. Page (ed.) Methods of soil analysis. Part 2. 2nd ed. Agron. Monogr. 9. ASA and SSSA, WI.

Norton, L.D. 1987. Micromorphological study of surface seals developed under simulated rainfall. Geoderma 40:127–140.

Poss, R., C. Pleuvret, and H. Saragoni. 1990. Influence des réorganisations superficielles sur l'infiltration dans les terres de Barre (Togo méridional). Cah. ORSTOM, ser. Pedol. 25:405–415.

Radcliffe, D.E., L.T. West, R.K. Hubbard, and L.E. Asmussen. 1991. Surface sealing in coastal plains loamy sands. Soil Sci. Soc. Am. J. 55:223–227.

Rawitz, E., W.B. Hoogmoed, and J. Morin. 1986. The effect of tillage practices on crust properties, infiltration and crop response under semi-arid conditions. p. 278–284. *In* Int. Symp. on the Assessment of Soil Surface Sealing and Crusting. Ghent, Belgium.

Rhoades, J.D. 1982. Cation exchange capacity. p. 149–157. *In* A.L. Page (ed.) Methods of soil analysis. Part 2. 2nd ed. Agron. Monogr. 9. ASA and SSSA, Madison, WI.

Russ, J.C. 1992. The image processing handbook. CRC Press, Boca Raton, FL.

Soil Survey Staff. 1992. Keys to soil taxonomy. Soil Manage. Support Serv. Tech. Monogr. 19. 5th ed. Pocahontas Press, Blacksburg, VA.

Sumner, M.E., and B.A. Stewart. 1992. Soil crusting: Chemical and physical processes. Advances in Soil Science, Lewis Publishers, Boca Raton, FL.

Tarchitzky, J., A. Banin, J. Morin, and Y. Chen. 1984. Nature, formation and effects of soil crusts formed by water drop impact. Geoderma 33:135–155.

Valentin, C. 1986. Surface crusting of arid sandy soils. p. 40–47. *In* Int. Symp. on the Assessment of Soil Surface Sealing and Crusting. Ghent, Belgium.

Valentin, C. 1991. Surface crusting in two alluvial soils of northern Niger. Geoderma 48:201–222.

Valentin, C., and L.-M. Bresson. 1992. Morphology, genesis and classification of surface crusts in loamy and sandy soils. Geoderma 55:225–245.

van der Watt, H.v.H., and C. Valentin. 1992. Soil crusting: The African view. p. 301–338. *In* M.E. Sumner and B.A. Stewart

(ed.) Soil crusting: Chemical and physical processes. Advances in Soil Science, Lewis Publishers, Boca Raton, FL.

West, L.T., J.M. Bradford, and L.D. Norton. 1990. Crust morphology and infiltrability in surface soils from the Southeast and Midwest U.S.A. p. 107–113. *In* L.A. Douglas (ed.) Soil micromorphology: A basic and applied science. Developments in Soil Science. Vol. 19. Elsevier Publ., Amsterdam, the Netherlands.

West, L.T., S.C. Chiang, and L.D. Norton. 1992. The morphology of surface crusts. p. 73–92. *In* M.E. Sumner and B.A. Stewart (ed.) Soil crusting: Chemical and physical processes. Advances in Soil Science, Lewis Publishers, Boca Raton, FL.

Whittig, L.D., and W.R. Allardige. 1986. X-ray diffraction techniques. p. 331–362. *In* A. Klute (ed.) Methods of soil analysis. Part 1. 2nd ed. Agron. Monogr. 9. ASA and SSSA, WI.